Improved Discrimination of Myocardial Perfusion Defects at Low Energy Levels Using Virtual Monochromatic Imaging

Patricia Carrascosa, MD, PhD, FSCCT, Alejandro Deviggiano, MD, Macarena de Zan, MD, Carlos Capunay, MD, Roxana Campisi, MD, and Gaston A. Rodriguez-Granillo, MD, PhD, FACC

Objectives: The aim of this study was to explore the diagnostic performance of dual-energy computed tomography perfusion (DE-CTP) at different energy levels.

Methods: Patients with known or suspected coronary artery disease underwent stress and rest DE-CTP and single-photon emission computed tomography. Images were evaluated using monochromatic data, and perfusion defects were initially identified in a qualitative manner and subsequently confirmed using attenuation levels.

Results: Thirty-six patients were included. Sensitivity, specificity, positive predictive value, and negative predictive value of DE-CTP for the identification of perfusion defects were 84.1%, 94.2%, 77.3%, and 96.2%, respectively. Perfusion defects showed significantly lower attenuation than normal segments, with the largest differences among low energy levels (sensitivity of 96% and specificity of 98% using a cutoff value ≤ 153 Hounsfield units at 40 keV), progressively declining at the higher levels ($P < 0.001$).

Conclusions: Dual-energy CTP at the lowest energy levels allowed improved discrimination of perfusion defects compared with higher energy levels.

Key Words: stress test, ischemia, cardiovascular diagnostic technics, multidetector computed tomography, coronary atherosclerosis

(*J Comput Assist Tomogr* 2017;41: 661–667)

Despite the consistently high diagnostic performance of computed tomography coronary angiography (CTCA) among patients with low to intermediate likelihood of coronary artery disease (CAD), patients with intermediate to high likelihood of CAD generally remain outside the diagnostic realm of this technique. This is primarily related to the challenging evaluation of segments with diffuse coronary calcification, potentially causing inconclusive or even false-positive findings.[1,2] Furthermore, the degree of luminal obstruction assessed either by CTCA or invasive coronary angiography has a weak relationship with the presence of inducible ischemia.[1] The extent of ischemia has been largely established as a predictor of events in patients with stable CAD; particularly, recent data suggest that revascularization improves the outcome only among patients with moderate to severe ischemia.[3,4] Overall, these data emphasize the importance of hemodynamic assessment in addition to the sole anatomic evaluation. Cardiac CT has therefore evolved accordingly, leading to the development of a number of strategies aimed at the evaluation of the functional significance of coronary stenosis.[5] The assessment of myocardial perfusion by CT (CTP) has been extensively validated both in animal models and in clinical studies. Several studies using diverse scanners, acquisition protocols, and pharmacological agents have demonstrated that stress CTP offers a significant incremental value over anatomical assessment alone by CTCA for the detection of ischemia.[6–10]

However, conventional single-energy CTP has limitations related to the polychromatic nature of the x-rays.[11] Virtual monochromatic imaging derived from dual-energy imaging (DE-CTP) has shown the ability to minimize some of these limitations. Nonetheless, the attenuation levels of perfusion defects assessed by DE-CTP remain poorly understood. Accordingly, we sought to explore the diagnostic performance and threshold attenuation levels of virtual monochromatic imaging at different energy levels for the detection of perfusion defects using DE-CTP.

MATERIALS AND METHODS

This prospective study involved patients with known or suspected CAD clinically referred for myocardial perfusion imaging by single-photon emission computed tomography (SPECT). All patients included were in sinus rhythm, were able to maintain a breath-hold for 15 seconds, and did not have a history of contrast-related allergy, renal failure, or hemodynamic instability. Additional exclusion criteria were patients younger than 18 years, a body mass index of greater than 32 kg/m^2, a history of previous myocardial infarction within the previous 30 days, percutaneous coronary revascularization within the previous 6 months, chronic heart failure, chronic obstructive pulmonary disease, high-degree atrioventricular block, or low estimated pretest probability of CAD (according to the Duke clinical score). Vasodilator medications were withdrawn for the previous 24 hours, and patients were advised to refrain from smoking and drinking caffeine beverages.

The protocol was approved by the institutional ethics committee, and all studies have been performed in accordance with the ethical standards as laid down in the 1964 Declaration of Helsinki and its later amendments. Informed consent was obtained from all individual participants included in the study.

CTP Acquisition

All patients were scanned using a dual-energy CT scanner equipped with garnet-based scintillator material detectors. Dual-energy imaging was performed by rapid switching (0.3–0.5 milliseconds) between low and high tube potentials (80–140 kV) from a single source (Discovery HD 750; GE Medical Systems, Milwaukee, Wis), enabling the reconstruction of low- and high-energy projections and the generation of monochromatic image reconstructions with 10-keV increments from 40 to 140 keV. Iterative reconstruction was applied at 40% adaptive statistical iterative reconstruction, from 60 to 140 keV because 60 keV is the lowest monoenergetic level available in our software version.

From the Department of Cardiovascular Imaging, Diagnóstico Maipú, Buenos Aires, Argentina.

Received for publication September 5, 2016; accepted November 18, 2016.

Correspondence to: Gaston A. Rodriguez-Granillo, MD, PhD, FACC, Av Maipú 1668, Vicente López (B1602ABQ), Buenos Aires, Argentina (e-mail: grodriguezgranillo@gmail.com).

Patricia Carrascosa is a consultant of GE Healthcare. None of the other authors have conflicts of interest to declare.

Supplemental digital contents are available for this article. Direct URL citations appear in the printed text and are provided in the HTML and PDF versions of this article on the journal's Web site (www.jcat.org).

DOI: 10.1097/RCT.0000000000000584

The same pharmacological stress was used for DE-CTP and SPECT scans. Dipyridamole (0.56 mg/kg) and iodinated contrast (iobitridol; Xenetix 350, Guerbet, France) were administrated using 2 independent antecubital intravenous lines. After dipyridamole infusion, aminophylline (1–2 mg/kg) was administrated intravenously to revert the vasodilator effect.

Stress DE-CTP was acquired using prospective electrocardiographic gating including 150 to 200 milliseconds of temporal padding aimed to cover approximately 40% to 75% of the R-R interval because systolic and diastolic phases were required for the analysis. Three minutes after dipyridamole administration, a dual-phase protocol with 50 to 70 mL of iodinated contrast followed by a 30- to 40-mL saline flush was injected through an arm vein. A bolus tracking technique was used to synchronize the arrival of contrast at the level of the coronary arteries with the start of the scan.

For rest DE-CTP, patients with a heart rate greater than 65 beats per minute received 5-mg intravenous propranolol if needed to achieve a target heart rate of less than 60 beats per minute. As only a mid-diastolic window was required for rest acquisitions, the scan was performed using a 100-millisecond padding centered at 75% of the cardiac cycle. Image acquisition at rest was executed after sublingual administration of 2.5 to 5 mg of isosorbide dinitrate.

SPECT Myocardial Perfusion Imaging

At the time of the stress DE-CTP, 2 minutes after dipyridamole administration and immediately before the CT scan, 10 to 15 mCi of technetium-99 m-methoxy isobutyl isonitrile were administrated. Stress SPECT image acquisition was performed 60 minutes after the administration of the radiotracer using a dual-head γ-camera over a 90° circular orbit (GE Medical Systems, Millennium MG, Milwaukee, Wis). Data were acquired in a 128 × 128 matrix for 32 projections in a step-and-shoot format. Rest SPECT image acquisition was completed within 24 to 48 hours after stress SPECT, after the administration of 10 to 15 mCi of technetium-99 m-methoxy isobutyl isonitrile.

DE-CTP Analysis

Computed tomography perfusion images were analyzed by a level 3–certified cardiac CT observer (PC), blinded to the clinical data, using a smooth filter in axial planes and multiplanar reconstructions. The evaluation of both DE-CTP and SPECT was performed using the American Heart Association (AHA) left ventricular 17-segment model, and segment 17 (apex) was excluded.[12] Short-axis views were obtained initially using 5-mm average multiplanar reconstructions from base to apex, with the full data set available for the reader. Images were evaluated using monochromatic data in gray scale and color scale. Different energy levels from 40 to 140 keV were applied, and the attenuation levels (in Hounsfield units [HU]) of the aforementioned 16 AHA segments were determined at each energy level. To validate a positive finding, it was required to identify a perfusion defect at all the energy levels explored. Using standardized regions of interest of 20 mm^2 localized at the interventricular septum over normally perfused myocardium (without perfusion deficits on any technique), myocardial attenuation level was determined. Myocardial perfusion defects were initially identified in a qualitative manner and subsequently confirmed if the involved attenuation level was 2 SDs less than the mean myocardial attenuation level. The dual-energy index (DEI) was also calculated between 80 and 140 keV and between 40 and 140 keV as previously reported: $(keV_a - keV_b) / (keV_a + keV_b + 2000)$.

After blind analyses of DE-CTP and SPECT findings, all segments (at stress and rest) were further categorized according to the combined presence of normal perfusion, perfusion defects (both positive), or discordant findings (1 positive). This enabled the comparison of the diagnostic performance between the different monochromatic energy levels using the segment-based quantitative data (Hounsfield units) for the detection of perfusion defects identified at both DE-CTP and SPECT.

Single-photon emission CT analysis was carried out by an experienced nuclear cardiologist (RC) blinded to the DE-CTP data. For that purpose, reconstruction into long- and short-axis projections perpendicular to the heart axis was initially performed, followed by an automated quantitative analysis of the perfusion images using polar map format (normalized to 100%). Myocardial perfusion defects were identified as segmental tracer activity less than 75% of maximum. Gated images were used to assess regional wall motion to enhance the discrimination between perfusion defects and attenuation artifacts.

Computed tomography effective radiation dose was derived by multiplying the dose-length product with the weighting (k) value of 0.014 mSv/mGy/cm for chest examinations, as suggested by the Society of Cardiovascular Computed Tomography.[13] Radiation dosimetry of SPECT was estimated based on recommendations of recently published guidelines.[14]

Statistical Analysis

Discrete variables are presented as counts and percentages. Continuous variables are presented as means (SD). Comparisons among groups were performed using 1-way analysis of variance (Bonferroni for multiple post hoc comparisons) or paired samples t tests. To determine the accuracy of DE-CTP for the detection of perfusion defects by SPECT, we calculated the sensitivity, specificity, positive predictive value, negative predictive value, and receiver operating characteristic (ROC) curve analyses on a per-patient and per-segment basis, accounting for potential nonuniform distribution (95% confidence intervals [CIs]). Receiver operating characteristic curve analyses were performed using specific software for ROC analysis (MedCalc Software, Ostend, Belgium). Pairwise comparisons of ROC curves were performed using the method of DeLong et al[15] for the detection of differences between 2 AUCs and calculated the binomial exact CI for the area under the curve. All other statistical analyses were performed using SPSS software, version 22.0 (Chicago, Ill). A 2-sided P value of less than 0.05 indicated statistical significance.

RESULTS

Demographics, Effective Dose Radiation, and Diagnostic Performance

This study included 38 patients who underwent stress/rest DE-CTP and SPECT imaging. Two patients were excluded because of severe motion artifacts. Twenty-five patients (69%) were men, and the mean (SD) age was 62.1 (11.4)years. Ten patients (28%) were diabetic, 27 (75%) had hypertension, and 26 (72%) had hypercholesterolemia. The mean (SD) body mass index was 28.0 (3.3)kg/m^2.

The mean (SD) heart rate during the acquisitions was 70.9 (11.4)beats per minute for stress DE-CTP and 58.5 (8.4)beats per minute for rest DE-CTP. No ischemic electrocardiographic changes were observed during pharmacological stress. The mean (SD) effective radiation dose was 4.9 (1.5)mSv with stress DE-CTP and 3.4 (0.6)mSv with rest DE-CTP (total, 8.3 [1.9]mSv). The mean (SD) effective radiation dose associated to SPECT was 5.0 (1.8)mSv with stress imaging and 4.8 (1.8)mSv with rest imaging (total, 9.8 [3.4]mSv). Paired differences in total effective

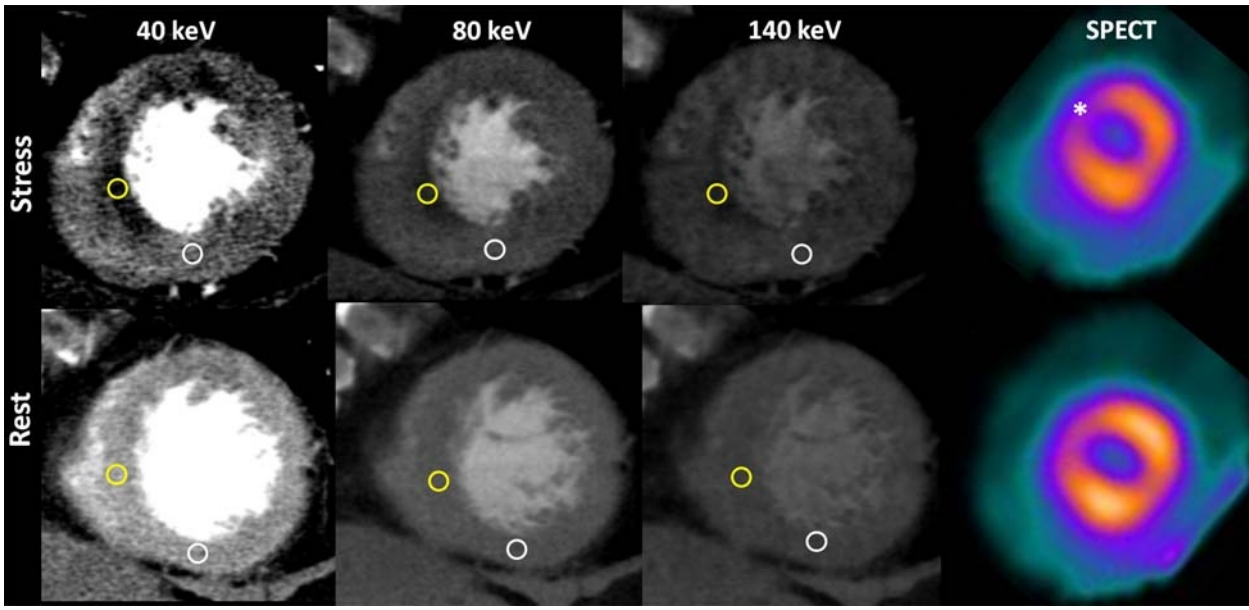

FIGURE 1. A 56-year-old male, former smoker, with effort angina. Heart rate at stress was 76 beats per minute, and heart rate at rest was 66 beats per minute. Presence of a reversible perfusion defect at the anterior and septal apical left ventricular wall (yellow). White regions of interests (ROIs) correspond to segment 15, where signal densities at stress/rest were 184 HU/215 HU (40 keV), 67 HU/84 HU (80 keV), and 43 HU/58 HU (140 keV). Yellow ROIs correspond to segment 14, where signal densities at stress/rest were 66 HU/194 HU (40 keV), 51 HU/64 HU (80 keV), and 43 HU/37 HU (keV). The reversible perfusion defect (*) is confirmed at SPECT. Figure 1 can be viewed online in color at www.jcat.org.

dose radiation associated with DE-CTP and SPECT were significant ($P = 0.004$).

Ten patients (28%) had no evidence of myocardial perfusion defects by CTP, 6 (17%) had 1 or more segments with fixed perfusion defects, 7 (19%) had 1 or more segments with reversible perfusion defects, and 13 patients (36%) had evidence of both fixed and reversible perfusion defects (Figs. 1, 2). All left ventricular segments were evaluated by DE-CTP among 11 incremental energy levels from 40 to 140 keV (during rest and stress). One segment was excluded because of severe artifacts. Overall, 424 segments (74%) had normal DE-CTP, 82 segments (14%) had fixed perfusion defects, and 68 segments (12%) had reversible perfusion defects.

On a per-segment basis, the sensitivity, specificity, positive predictive value, and negative predictive value of DE-CTP for the identification of perfusion defects were 84.1% (95% CI, 79%–89%), 94.2% (95% CI, 93%–96%), 77.3% (95% CI, 71%–82%), and 96.2% (95% CI, 95%–97%). On a per-patient basis, the sensitivity, specificity, positive predictive value, and negative predictive value of DE-CTP for the identification of perfusion defects were 91.3% (95% CI, 72%–99%), 61.5% (95% CI, 32%–86%), 80.8% (95% CI, 61%–93%), and 80.0% (95% CI, 44%–97%).

Attenuation Levels of Normally Perfused Segments and of Segments With Fixed and Reversible Perfusion Defects

Overall, attenuation levels and image noise were significantly higher at the lowest energy levels, gradually declining at increasing energy levels (Figs. 3–5). Signal-to-noise ratio was highest at 70 and 80 keV (3.8 [2.0] in both), whereas it was significantly lower

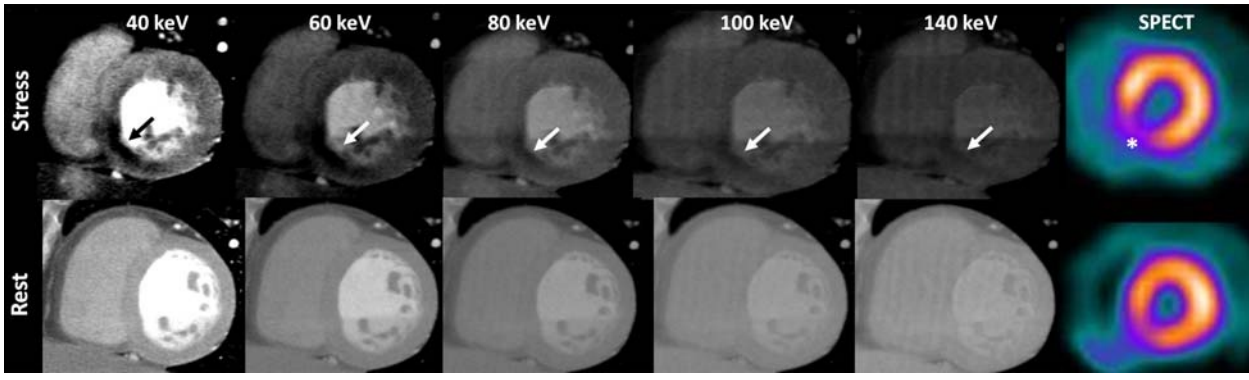

FIGURE 2. A 48-year-old woman, with hypertension, hypercholesterolemia, and smoking as coronary risk factors. Heart rate at stress was 78 beats per minute, and heart rate at rest was 61 beats per minute. A reversible perfusion defect at the inferoseptal left ventricular wall (arrows) is observed more clearly at the lower energy levels, with almost complete normalization at rest. Single-photon emission CT images confirm the findings (*). Figure 2 can be viewed online in color at www.jcat.org.

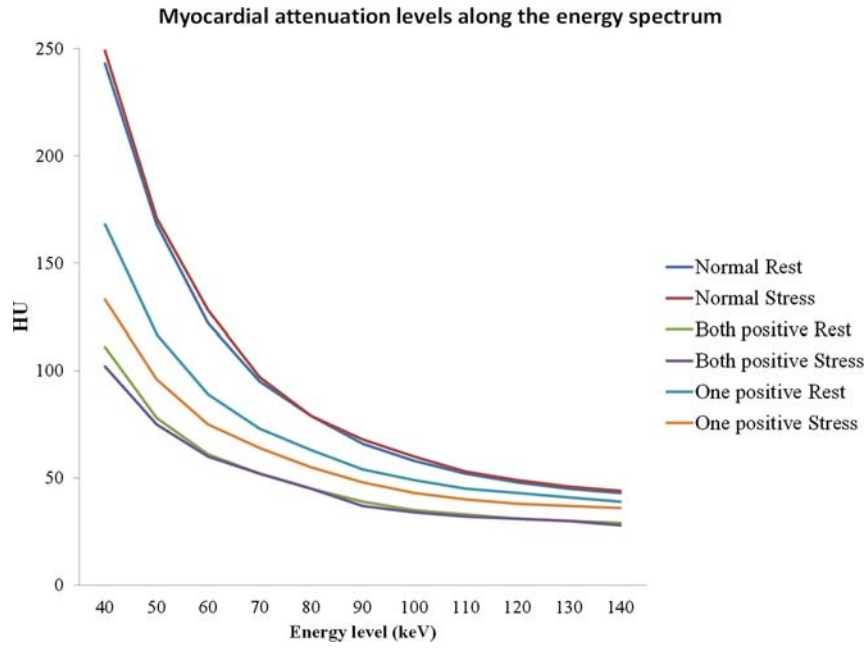

FIGURE 3. Attenuation levels (Hounsfield units) of myocardial segments with normal perfusion, in segments with abnormal myocardial perfusion identified with both CTP and SPECT, and in segments with discordant findings (SPECT or CTP positive). Figure 3 can be viewed online in color at www.jcat.org.

at the lowest and highest energy levels (40 keV, 2.8 [1.5] and $P < 0.0001$ vs 70 keV; 140 keV, 2.8 [1.9] and $P < 0.0001$ vs 70 keV).

Segments with normal perfusion during either rest or stress showed similar signal attenuation levels and were significantly higher than segments with perfusion defects. Such differences remained significant across the different energy levels ($P < 0.0001$), although they progressively declined at higher energy levels (Figs. 1, 2; Tables, Supplemental Digital Content 1, http://links.lww.com/RCT/A60). Furthermore, the attenuation levels of both fixed and reversible defects (during stress) did not differ across low energy and mid-energy levels (40 keV, $P = 1.0$; 80 keV, $P = 0.06$ [Bonferroni]), whereas significant differences were identified at the highest energy level (140 keV, $P < 0.0001$ [Bonferroni]).

The largest attenuation differences between segments with normal perfusion and those with perfusion defects (identified both at DE-CTP and SPECT) were observed among low energy levels (sensitivity of 96% and specificity of 98% using a cutoff value ≤

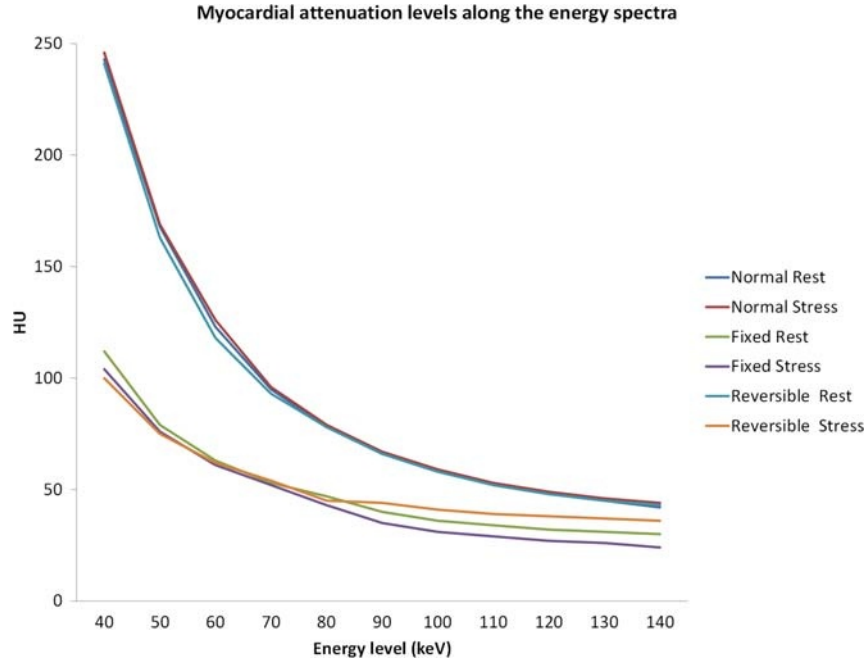

FIGURE 4. Attenuation levels (Hounsfield units) of myocardial segments with normal CTP, in segments with fixed defects assessed by CTP, and in segments with reversible perfusion defects assessed by CTP. Figure 4 can be viewed online in color at www.jcat.org.

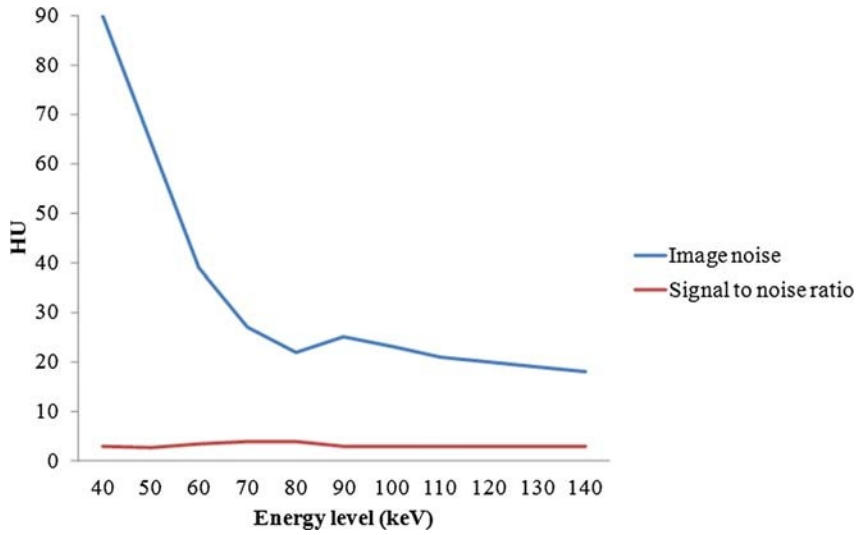

FIGURE 5. Myocardial image noise and signal-to-noise ratio across different energy levels. Figure 5 can be viewed online in color at www.jcat.org.

153 HU at 40 keV), progressively declining at the highest energy levels (area under the ROC curve of 40 keV, 0.98 [95% CI, 0.97–0.99] vs 80 keV, 0.94 [95% CI, 0.93–0.96] vs 140 keV, 0.73 [95% CI, 0.70–0.76]; $P < 0.001$ for all comparisons). Such differences are further portrayed in Figure 6. The diagnostic performance of the DEI 40–140 for the detection of perfusion defects was significantly higher than with using the DEI 80–140 (area under the ROC curve of DEI 40–140, 0.97 [95% CI, 0.96–0.98] vs DEI 80–140, 0.89 [95% CI, 0.87–0.91]; $P < 0.001$), with a sensitivity of 90% and a specificity of 97% using a cutoff value of 0.054 or less.

Finally, the segments most commonly affected by beam-hardening artifacts (BHAs) (AHA-5 and AHA-13) showed a similar myocardial attenuation than segments with normal myocardial perfusion (see Tables, Supplemental Digital Content 1, http://links.lww.com/RCT/A60).

DISCUSSION

The main finding of our study was that virtual monochromatic imaging at the lowest energy levels derived from DE-CTP allowed more accurate discrimination of perfusion defects compared with higher energy levels.

We identified 40 keV as the energy level with the highest diagnostic performance for the detection of perfusion defects, with a sensitivity of 96% and a specificity of 98% for a threshold value of 153 HU or less. In turn, the diagnostic performance of virtual monochromatic analysis of DE-CTP progressively declined at the highest energy levels. Indeed, the clear differences observed at the lowest energy levels were conflicting at 140 keV. This might be partially related to the virtual absence of contrast enhancement in these reconstructions. Such inconsistent finding is further portrayed by the significant differences identified between fixed and reversible defects (during stress) at 140 keV. Nonetheless, mid-energy levels might still be necessary to rule out the presence of BHAs because previous studies have shown that those located at the posterobasal wall tend to fade away at higher (≥70 keV) energy levels.[16] In this study, the left ventricular segments most commonly affected by BHA showed similar attenuation levels than segments with normal myocardial perfusion.

In keeping with previous data, the highest attenuation levels achieved at 40 keV were at the expense of significantly higher image noise. It is noteworthy that the latest iterative reconstruction algorithms will allow a considerable noise reduction also for less than 60 keV. In parallel, a recent study has suggested that the application of advanced noise-optimized virtual monochromatic imaging algorithms can significantly improve the image quality of DE-CT acquisitions.[17]

Finally, there has been previously some insinuation that ischemia might be detected at the lowest energy levels without the need for stress imaging. This speculative hypothesis was refuted in our study because the attenuation levels at rest were similar between segments with normal perfusion and those with ischemia.

Despite its recognized excellent negative predictive value, the specificity and positive predictive value of CTCA might be suboptimal, particularly among patients at intermediate to high risk of CAD, who are likely to have diffuse coronary calcification.[1,2] Such limitation can occasionally lead to an increment in the rate of downstream diagnostic tests including the risk of unnecessary referral to invasive coronary angiography.[18] Pharmacological stress CTP, extensively validated in both animal and clinical studies, has emerged as a means to overcome most of these limitations by exploring the hemodynamic significance of lesions.[5] Computed tomography perfusion can be assessed using 2 distinct strategies: static or dynamic. Briefly, static CTP involves

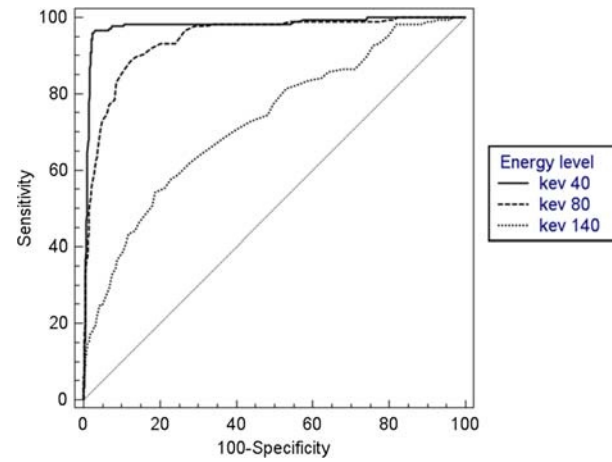

FIGURE 6. Receiver operating characteristic curves of DE-CTP at different energy levels for the detection of perfusion defects. Figure 6 can be viewed online in color at www.jcat.org.

a single acquisition during first-pass enhancement, allowing a mainly qualitative evaluation of myocardial perfusion based on the attenuation levels of the differences between normal and ischemic areas. Conversely, dynamic CTP enables a quantitative estimation of myocardial perfusion by the generation of time-attenuation curves and absolute myocardial blood flow derived from multiple sequential CT data sets. Nevertheless, dynamic CTP is related to significantly higher radiation doses compared with static CTP.[19] Anyhow, there is a good agreement between both strategies, sharing a high diagnostic performance for the detection of perfusion defects.[20]

One of the core limitations of CTP are BHAs, which are related to the polychromatic nature of x-rays and the energy dependency of x-ray attenuation and can mimic perfusion defects.[11] Dual-energy CTP has demonstrated the ability to mitigate BHA through the generation of virtual monochromatic image reconstruction, adding an incremental value over coronary anatomy for the detection of ischemia in patients with intermediate to high CAD likelihood and with improved diagnostic performance over conventional single-energy CTP.[21–25]

Furthermore, DE-CTP has shown improved diagnostic performance for the assessment of myocardial perfusion as compared with single-energy CTP, mostly attributed to the ability of DE-CTP to attenuate the presence of BHA.[21]

As DE-CTP is based on the myocardium contrast attenuation, it is pivotal to establish threshold attenuation levels for normal, ischemic, and necrotic myocardium for each energy level. The energy thresholds for the distinction between normal CTP and BHA have been previously established, whereas the attenuation levels of perfusion defects at different energy levels remain poorly explored.

Overall, our results provide some reference regarding the boundaries beyond which attenuation levels drop during DE-CTP, which might be interpreted as a perfusion defect. Furthermore, in line with previous studies, we identified a significantly lower effective radiation dose with DE-CTP compared with SPECT. Future studies should explore whether these data could be applied for the development of automatic CTP algorithms.

Limitations

A number of limitations should be acknowledged. Because the sample size was relatively small, potential selection bias cannot be fully excluded. Patients did not undergo invasive coronary angiography; therefore, confirmation of the presence of obstructive CAD by means of stress SPECT is potentially subject to error. Finally, data regarding infarct age were not available, and late enhancement acquisitions were performed only in a limited number of patients. In this regard, it is noteworthy that myocardial attenuation values of fixed defects were similar than those of reversible perfusion defects, suggesting that adipose tissue within healed myocardium was limited or absent.[26]

CONCLUSIONS

In this study, virtual monochromatic imaging at the lowest energy levels derived from DE-CTP allowed a more accurate discrimination of perfusion defects compared with higher energy levels.

REFERENCES

1. Meijboom WB, van Mieghem CA, Mollet NR, et al. 64-slice computed tomography coronary angiography in patients with high, intermediate, or low pretest probability of significant coronary artery disease. *J Am Coll Cardiol*. 2007;50:1469–1475.
2. Vavere AL, Arbab-Zadeh A, Rochitte CE, et al. Coronary artery stenoses: accuracy of 64-detector row CT angiography in segments with mild, moderate, or severe calcification—a subanalysis of the CORE-64 trial. *Radiology*. 2011;261:100–108.
3. Shaw LJ, Iskandrian AE. Prognostic value of gated myocardial perfusion SPECT. *J Nucl Cardiol*. 2004;11:171–185.
4. Hachamovitch R, Hayes SW, Friedman JD, et al. Comparison of the short-term survival benefit associated with revascularization compared with medical therapy in patients with no prior coronary artery disease undergoing stress myocardial perfusion single photon emission computed tomography. *Circulation*. 2003;107:2900–2907.
5. Gonçalves Pde A, Rodríguez-Granillo GA, Spitzer E, et al. Functional evaluation of coronary disease by CT angiography. *JACC Cardiovasc Imaging*. 2015;8:1322–1335.
6. George RT, Arbab-Zadeh A, Miller JM, et al. Computed tomography myocardial perfusion imaging with 320-row detector computed tomography accurately detects myocardial ischemia in patients with obstructive coronary artery disease. *Circ Cardiovasc Imaging*. 2012;5:333–340.
7. Bettencourt N, Rocha J, Ferreira N, et al. Incremental value of an integrated adenosine stress-rest MDCT perfusion protocol for detection of obstructive coronary artery disease. *J Cardiovasc Comput Tomogr*. 2011;5:392–405.
8. Ko SM, Choi JW, Hwang HK, et al. Diagnostic performance of combined noninvasive anatomic and functional assessment with dual-source CT and adenosine-induced stress dual-energy CT for detection of significant coronary stenosis. *AJR Am J Roentgenol*. 2012;198:512–520.
9. Bamberg F, Marcus RP, Becker A, et al. Dynamic myocardial CT perfusion imaging for evaluation of myocardial ischemia as determined by MR imaging. *JACC Cardiovasc Imaging*. 2014;7:267–277.
10. Cury RC, Kitt TM, Feaheny K, et al. A randomized, multicenter, multivendor study of myocardial perfusion imaging with regadenoson CT perfusion vs single photon emission CT. *J Cardiovasc Comput Tomogr*. 2015;9:103–112.
11. Rodríguez-Granillo GA, Rosales MA, Degrossi E, et al. Signal density of left ventricular myocardial segments and impact of beam hardening artifact: implications for myocardial perfusion assessment by multidetector CT coronary angiography. *Int J Cardiovasc Imaging*. 2010;26:345–354.
12. Cerqueira MD, Weissman NJ, Dilsizian V, et al. Standardized myocardial segmentation and nomenclature for tomographic imaging of the heart. A statement for healthcare professionals from the Cardiac Imaging Committee of the Council on Clinical Cardiology of the American Heart Association. *Int J Cardiovasc Imaging*. 2002;18:539–542.
13. Halliburton SS, Abbara S, Chen MY, et al. SCCT guidelines on radiation dose and dose-optimization strategies in cardiovascular CT. *J Cardiovasc Comput Tomogr*. 2011;5:198–224.
14. Dorbala S, Di Carli MF, Delbeke D, et al. SNMMI/ASNC/SCCT guideline for cardiac SPECT/CT and PET/CT 1.0. *J Nucl Med*. 2013;54:1485–1507.
15. DeLong ER, DeLong DM, Clarke-Pearson DL. Comparing the areas under two or more correlated receiver operating characteristic curves: a nonparametric approach. *Biometrics*. 1988;44:837–845.
16. Rodriguez-Granillo GA, Carrascosa P, Cipriano S, et al. Beam hardening artifact reduction using dual energy computed tomography: implications for myocardial perfusion studies. *Cardiovasc Diagn Ther*. 2015;5:79–85.
17. Albrecht MH, Trommer J, Wichmann JL, et al. Comprehensive comparison of virtual monoenergetic and linearly blended reconstruction techniques in third-generation dual-source dual-energy computed tomography angiography of the thorax and abdomen. *Invest Radiol*. 2016;51:582–590.
18. Nielsen LH, Ortner N, Norgaard BL, et al. The diagnostic accuracy and outcomes after coronary computed tomography angiography vs. conventional functional testing in patients with stable angina pectoris: a systematic review and meta-analysis. *Eur Heart J Cardiovasc Imaging*. 2014;15:961–971.

19. Rossi A, Merkus D, Klotz E, et al. Stress myocardial perfusion: imaging with multidetector CT. *Radiology*. 2014;270:25–46.

20. Feuchtner G, Goetti R, Plass A, et al. Adenosine stress high-pitch 128-slice dual-source myocardial computed tomography perfusion for imaging of reversible myocardial ischemia: comparison with magnetic resonance imaging. *Circ Cardiovasc Imaging*. 2011;4:540–549.

21. Carrascosa PM, Cury RC, Deviggiano A, et al. Comparison of myocardial perfusion evaluation with single versus dual-energy CT and effect of beam-hardening artifacts. *Acad Radiol*. 2015;22: 591–599.

22. Weininger M, Schoepf UJ, Ramachandra A, et al. Adenosine-stress dynamic real-time myocardial perfusion CT and adenosine-stress first-pass dual-energy myocardial perfusion CT for the assessment of acute chest pain: initial results. *Eur J Radiol*. 2012;81:3703–3710.

23. Ruzsics B, Lee H, Zwerner PL, et al. Dual-energy CT of the heart for diagnosing coronary artery stenosis and myocardial ischemia-initial experience. *Eur Radiol*. 2008;18:2414–2424.

24. Carrascosa PM, Deviggiano A, Capunay C, et al. Incremental value of myocardial perfusion over coronary angiography by spectral computed tomography in patients with intermediate to high likelihood of coronary artery disease. *Eur J Radiol*. 2015;84:637–642.

25. De Cecco CN, Harris BS, Schoepf UJ, et al. Incremental value of pharmacological stress cardiac dual-energy CT over coronary CT angiography alone for the assessment of coronary artery disease in a high-risk population. *AJR Am J Roentgenol*. 2014;203:W70–W77.

26. Rodríguez-Granillo GA, Rosales MA, Renes P, et al. Chronic myocardial infarction detection and characterization during coronary artery calcium scoring acquisitions. *J Cardiovasc Comput Tomogr*. 2010;4:99–107.